Int. J. Heat Mass Transfer. Vol. 36, No. 7, pp. 1923–1941, 1993
Printed in Great Britain

0017-9310/93 $6.00 + 0.00

The role of buoyant thermals in salt gradient solar ponds and in convection more generally

LESLIE B. MULLETT
42 Grosvenor Avenue, Bourne, Lincs PE10 9HU, U.K.

(*Received* 17 *October* 1991 *and in final form* 27 *August* 1992)

Abstract—A salt gradient solar pond is a large thermo-haline double-diffusive system of depth up to 3 m, having a lower convecting or storage zone with about 20% salt by weight, and a non-convecting uniform-gradient zone above providing insulation. Heating by solar radiation is partly within the liquid and partly at the base. The principal fluid mechanics problems are growth of the lower convecting zone, emergence and growth of an upper convecting zone and the possible breakdown of the gradient zone into a number of convecting zones *simultaneously*. It is shown that the well accepted model of double-diffusive convection for 'strong' heating from below a stable salinity gradient does not apply at the very modest level of solar radiation, more especially when part (or even all) of the heat is generated within the fluid. New models are developed in which buoyant thermals play causal roles (as, indeed, they do in the case of 'strong' heating). Thermals from all three kinds of boundaries are investigated, and it is found that although there is a limited quantity of fluid in a thermal, connection is retained with the source during its lifetime. Thermals from the solid base are of the well known axisymmetric kind. Those from the boundary with air, and from liquid of a different density, the so-called 'free' boundaries, are shown to be two-dimensional and Gaussian in profile. Thermal ranges are found to be well defined and increase according to environmental (water) temperature, with a common form of range equation. The equation is calibrated experimentally for each type of thermal. For a given environmental temperature, axisymmetric thermals have by far the longest range whilst Gaussian thermals from a boundary with air have the shortest. If thermals do not reach the opposite boundary there is local heating or cooling; if they do, there is boundary erosion and zone growth, that is, penetrative convection. Each convecting zone has two sets of thermals, upwards and downwards, which are the principal means of heat transfer. This is illustrated for the particular case of a solar pond. Finally, it is shown that the onset of 'turbulence' at Rayleigh numbers in the region of 5×10^4 to 10^5 marks the transition from laminar Bénard–Rayleigh heat flow to quantised flow by thermals.

1. INTRODUCTION TO SOLAR PONDS AND MODELLING

THE SALT gradient solar pond is simple in principle and many examples occur in nature, such as the Medve Lake in Transylvania and lakes in the Carpathian Mountains of northern Romania. Bottom temperatures reach up to 70°C due to the remarkable properties of salt water. With a high concentration of salt at the bottom and a sufficiently uniform gradient to zero or near zero at the top, buoyancy is overcome and convection suppressed. Water is then a good thermal insulator; one metre being equivalent to 2–3 cm of foam plastic insulation. Afeef [1] and Afeef and Mullett [2] have shown that even when loaded with 20% of sodium and/or magnesium chloride, water will settle and clear to the transparency of distilled water for the shorter wavelengths of the solar spectrum. Of the total insolation, about 25% is infrared which is absorbed right at the surface, whilst 20–30% reaches a depth of several metres.

During the 1960s, the potential of artificial ponds was recognised for the efficient and economic collection and storage of solar energy. Pioneering work owes much to Rabl and Nielsen [3] in the United States and to Weinberger [4] and Tabor [5] in Israel. Development has spread around the world, especially to those areas having excellent insolation conditions, such as the Middle East generally, Australia and South America. Commercial scale exploitation is most advanced in Israel where strategic energy considerations make it desirable to use the resultant water at 80–90°C for electricity generation.

Artificial ponds, Fig. 1, have a total depth of 2–3 m. The lower convecting (or storage) zone is about 1 m in depth and is laid down with a concentration of the order of 20% by weight of sodium and/or magnesium chloride. In the gradient zone above, with a depth of about 1.5 m, the salt concentration is reduced as near linearly as possible, to zero or a low value at the surface. After the 25% infrared has been absorbed in the first few millimetres, the rest of the solar radiation is absorbed roughly equally within the fluid and at the base.

In fluid mechanics terms, the pond is a large thermo-haline double-diffusive system whose performance is governed by the vertical gradients of temperature and salt concentration and their diffusivities. Maintenance is required to sustain the salt gradient against salt diffusion. On heating, the principal fluid mechanics problems are growth of the lower convecting zone, the appearance and growth of an upper convecting

NOMENCLATURE

A	thermal fluid area
d	fluid depth
erf	error function
erfc	1 − erf complementary error function
g	acceleration due to gravity
G	constant for a type of thermal, $\delta^2 r^2(\Delta T/2)$
H	heat flux
K	thermal diffusivity
K_s	diffusivity of salt
K_T	diffusivity of heat
M	Marangoni number
$M - d/\delta$	nondimensional height
n	vertical wave number
N	flux of thermals
N	angular frequency of buoyancy oscillation
Nu	Nusselt number
Pr	Prandtl number
r	radial distance over which velocity and temperature difference fall to zero
Ra	Rayleigh number
Ra_c	critical Rayleigh number
R_s	salinity Rayleigh number
s	salinity
t	time
T	temperature
V	thermal volume
w	power [watts]
z	vertical height in pond
Z	thermal range.

Greek symbols

α	thermal expansion coefficient
α	horizontal wave number
γ	surface tension
δ	boundary layer thickness
δ	characteristic dimension
ΔT	temperature difference
μ	molecular viscosity
ν	kinematic viscosity
ρ	fluid density
ρ'	density difference in a thermal
σ	Prandtl number.

zone, and possible breakdown of the gradient zone into a number of convecting zones, *simultaneously not sequentially*.

These problems are far more readily studied in laboratory models than 'in the field', but the consequences of scaling are different in each case. Reduction of the vertical dimensions gives direct information about stability of the gradient zone since both temperature and salinity gradients are scaled. Growth of the lower convecting zone requires experimental calibration of an analytical model to extrapolate to actual pond dimensions. For power input similar to solar conditions, thermal build-up time is reduced by the vertical scaling, but further reduction by increased power input can lead to quite different phenomena. This is so in respect of breakdown of the gradient zone. The upper convecting zone is a surface phenomenon unaffected by scaling.

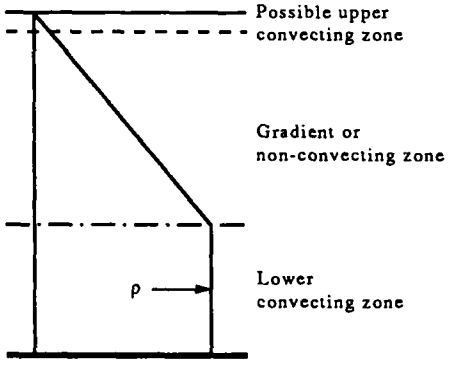

FIG. 1. Schematic of salt gradient solar pond.

2. GROWTH OF THE LOWER CONVECTING ZONE

2.1. *Modelling*

The programme of modelling work at the University of Reading was pioneered by Tsilingiris [6]. Well insulated metal and plastic vessels were used around 40 cm in diameter. They were filled to a depth of about 47 cm with clear water with a linear gradient of sodium chloride. The concentration was varied from various maximum values at the bottom to zero at the top. Heat was supplied by a solar simulation lamp, equivalent at its maximum rating to about 'one sun' continuously. After absorption of the infrared at the top, the majority of energy release was at the blackened bottom.

Temperature and density were measured and recorded simultaneously as a function of height. For the purpose, Tsilingiris developed a direct buoyancy/density meter. A silica rod, typically of 4 mm diameter and 5 cm in length, was suspended horizontally from a fine nylon line attached to a sensitive load cell. Since silica has a negligible coefficient of expansion with temperature, the amplified output was directly related to the density of the displaced fluid. The whole device, together with a thermocouple at the same height as

the rod, was mounted and traversed vertically on a motorised lead-screw. Typical scan time was about two minutes. It has since been discovered that Richards [7] had earlier utilised the principle with a glass tube partially sealed with paraffin wax and suspended horizontally from a balance.

In all the runs, using a wide range of maximum salt concentrations up to near saturation, Tsilingiris observed the immediate emergence and growth of a lower convecting zone. Growth ceased immediately the power source was switched off. It was found that the growth rate increased with increased simulator power and with decreased salt concentration. But growth rate for typical solar radiation was far less than that of the 'strong' heating from the base necessary to achieve the double-diffusive criterion of Turner [8, 9]. This requires that the applied heat be virtually confined to the lower convecting zone, that is, with a temperature discontinuity to the remaining gradient zone. The reduction in density in the convecting zone due to the temperature rise is just balanced by the increase due to mixing of the salt, leaving no step in density to the gradient zone. Yet in the solar pond models there was always a gradient of temperature into the salt gradient zone and a step in density, as shown, for example, in Tsilingiris and Mullett [10] and in Fig. 2 by Azhari [11]. Temperature fluctuations were observed at the boundary between the lower convecting zone and the gradient zone, with two characteristic frequencies of about five cycles per minute and one cycle in five minutes. But there was no evidence of anomalous behaviour, such as a threshold or saturation, which might have given a clue as to the mechanism involved. According to available knowledge at that time some form of penetrative convection was considered to be responsible, as sought analytically by fluid dynamicists such as Veronis [12] and, later, by solar pond investigators such as Zangrando *et al.* [13].

Azhari [11] made the first observations of the possible role of buoyant thermals. Solar pond models of similar diameter were filled to a depth of 36 cm, but with electrical heating at the base and a more developed model of the Tsilingiris scanner and associated electronics. With average power at the base of 300 W m^{-2}, successive runs were carried out at maximum salt concentrations of 5, 10, 15 and 20% by weight. A slowing down of growth rate of the lower convecting zone was observed but with no apparent threshold or distinct saturation. The 15% run was repeated at 150 and 450 W m^{-2}. Growth rate increased with power input but not in any distinctive way. Conditions were not pressed to breakdown of the gradient zone.

A typical set of temperature and density scans with advancing time is shown in Fig. 2. There were apparent temperature fluctuations at the zone boundary, at much the same frequencies found by Tsilingiris, due to movement of fluid at temperatures different from the brackground. However, with the more sensitive density probe, at high gain, strong and rapid fluctuations were observed within the lower convecting

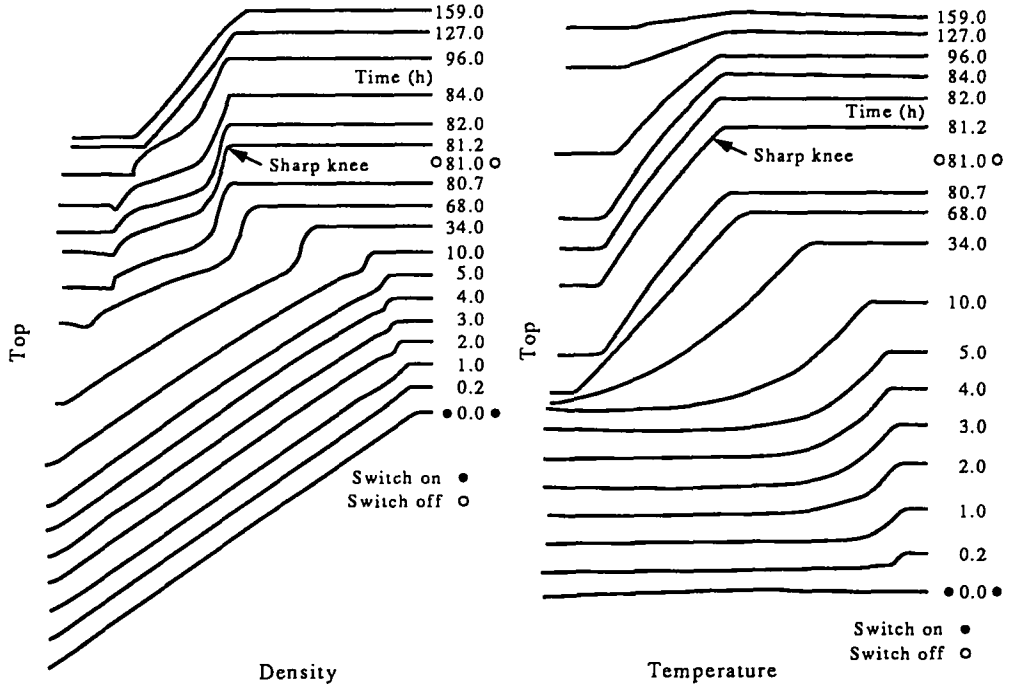

FIG. 2. Vertical distributions of density and temperature in a solar pond model (Azhari [11]).

zone, suggestive of impulses from locally turbulent upward movement of fluid. This was confirmed by the still larger impulses observed with a flat disc of silica of the same volume as the rod. The impulses appeared within a minute of switching on the heater and disappeared equally rapidly on switching off, strongly suggestive of thermals from the heated base striking the disc. The introduction of a layer of dye onto the base, using as dilutant some salt solution extracted from the bottom, revealed such thermals beginning to rise very soon after switching on. They ceased immediately on switching off. Although tending to wander before being stopped by the density step at the gradient zone, they were seen to be much longer versions of the axisymmetric thermals photographed by Sparrow *et al.* [14]. Evidence of mixing was noted at the boundary with the gradient zone, both density and temperature scans becoming rounded as heating was applied and reverting to being sharp when it was removed.

Measurements with dye in a deep glass tank heated at the base and filled with 15% salt solution showed that the thermals appeared to have very roughly constant velocity and quite distinct range increasing with environmental (fluid) temperature. They retained connection with their points of origin during their lifetime, appearing more like the 'starting plumes' of Turner [9] (p. 166). *Increased power input increased the rate of thermal formation without obvious effect on appearance.* At a fluid temperature of 20°C, the velocity was about 6 mm s^{-1}, making the thermals immediately recognisable against any background of dye. The range was about 44 cm.

A simplified model pond was set up with a lower zone of 44 cm of uniform 15% salt solution with plain water above. Starting at 15°C, the density/temperature probe showed no growth of the lower zone, but at 20°C, growth became rapid. The best estimate of the temperature at which the thermals reached a range of 44 cm was 17°C. More fundamental study was clearly required of axisymmetric thermals and their ranges as a function of environmental temperature, preferably with an analytical model to extrapolate to actual solar pond conditions of height and temperature.

2.2. *The origin of thermals*

Heat transfer by conduction from a moderately heated base involves a temperature distribution advancing with time as

$$T = \frac{\Delta T}{2}[1 - \mathrm{erf}\,\{z/2 \cdot \sqrt{(K \cdot t)}\}] \qquad (1)$$

where $\Delta T/2$ is the temperature difference between the fluid and the base, z the vertical height, t the time and K the thermal diffusivity. As with an exponential, an effective wavefront can be defined by extrapolating the gradient at $z = 0$ until it reaches the z axis at $\delta = \sqrt{(\pi K t)}$. The value of $2T/\Delta T$ is then 0.21. δ is assumed to be the boundary layer thickness and the heat flux is proportional to $1/\delta$.

There is a strong tendency to overturn, given an initial perturbation. It is generally believed that this occurs at a time t^* when an appropriate critical value of Rayleigh number is reached for the boundary layer,

$$Ra_c = g\frac{\alpha}{Kv} \cdot \delta^3 \frac{\Delta T}{2}$$

where g is the acceleration due to gravity, α the coefficient of expansion and v the kinematic viscosity.

Howard [15] was particularly concerned with a solid horizontal boundary in air. He assumed $Ra_c \sim 10^3$. At the corresponding time t^* the *whole* of the buoyant fluid in the boundary layer was considered to break away in a short time compared with t^*. The process was then repeated. The time averages of the conduction profile were computed over the time interval $(0, t^*)$ and showed good agreement with the mean temperature profile in the lower atmosphere measured by Townsend [16]. Figure 3 is based on Turner [9]. However, whereas the breakaway of buoyant fluid over a wide area is consistent with the form of thermals in the atmosphere, it is certainly not so for thermals from a solid lower boundary in water or an aqueous solution. High spots of thermal conductivity trigger the emission of buoyant fluid as axisymmetric thermals.

Elder [17] observed this phenomenon in a two-dimensional computer model. Initially, a first exponential was triggered by an applied surface imperfection, followed by a second exponential amplification phase. The final phase, Fig. 4, was the emission of a blob of buoyant fluid, only *partially* denuding that region of the boundary. Although the characteristic dimension of the blob was of the order of thickness of the boundary layer, the majority of the fluid could be seen to be from the leading edge. This would be even more accentuated in three dimensions, and seems to be confirmed by some experimental

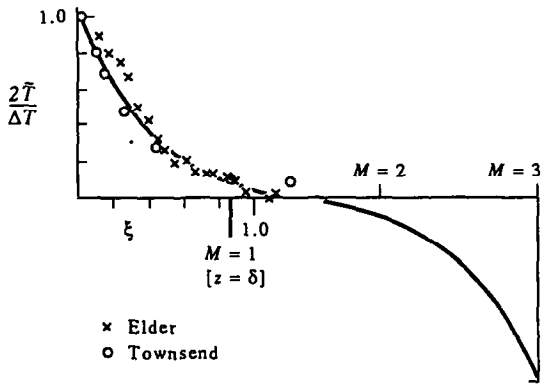

FIG. 3. Mean temperature profile of boundary layer (based on Howard [15]).

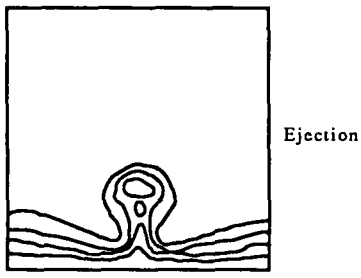

FIG. 4. Two dimensional growth of a thermal from a metal base—showing isothermals (Elder [17]).

results for water due to Elder shown by Turner [9] in Fig. 3. The distinctly higher mean temperatures near the boundary, shown by the crosses, imply that less fluid from this region is being stripped away in thermals. Elder also computed the case of a spacially periodic perturbation over the boundary, leading to the simultaneous ejection of a corresponding row of thermals.

Elder used (quote) "a critical Rayleigh number, which for want of a better choice, we take as the value given by the corresponding Bénard–Rayleigh problem", that is a value of 1100, as appropriate between a solid surface and a 'free' or density difference surface. The corresponding value of δ for an environmental temperature of 20°C and $\Delta T/2$ of 1°C is 4.29 mm.

2.3. *A range equation*

Initial calculations of the behaviour of a blob of fluid in water included inertial effects, but this proved unnecessary since constant velocity was very soon reached due to viscous drag. Ideally, a simple equation of state was required which could be calibrated and checked with measured data, and used to extrapolate with temperature and height to actual solar ponds. Turner [9] had devised just such an equation, to illustrate convection and Rayleigh number. He used a single characteristic dimension δ for *all* the dimensions involved. Calibration takes care of them all. There is, however, some advantage in distinguishing between δ as the characteristic dimension of the blob of fluid and r, the radial distance over which velocity and temperature difference fall to zero.

Equating buoyancy force and viscous drag:

$$g\rho' V = \mu \frac{A}{r} \cdot \frac{dz}{dt}$$

where ρ' is the density difference of the fluid in the thermal, V the fluid volume, μ the molecular viscosity, A the fluid surface area and r the radial distance over which dz/dt falls to zero.

The rate of reduction of ρ' is related to the thermal diffusivity as

$$\frac{d\rho'}{dt} = -K\frac{\rho' A}{Vr}.$$

Hence

$$\rho' = \rho'_0 \exp\left(-Kt\frac{A}{Vr}\right)$$

$$\frac{dz}{dt} = g\frac{V}{A}\frac{r}{\mu}\rho'_0 \exp\left(-Kt\frac{A}{Vr}\right).$$

Integrating over time from 0 to ∞

$$z = g\frac{V^2}{A^2}\frac{r^2}{K\mu}\cdot\rho'_0 \quad \mu = \nu\rho \quad \rho'_0 = \frac{d\rho}{dT}\cdot\frac{\Delta T}{2}$$

$$= g\frac{\alpha}{K\nu}\cdot\frac{V^2r^2}{A^2}\cdot\frac{\Delta T}{2} \quad \alpha = \text{coefficient of expansion.}$$

For axisymmetric thermals:

$$V \sim \delta^3 \quad A \sim \delta^2 \quad \frac{V^2}{A^2} \sim \delta^2.$$

Writing $G = \delta^2 r^2(\Delta T/2)$ the range equation becomes

$$Z = g\frac{\alpha}{K\nu}\cdot G. \tag{2}$$

This form is ideal for calibration since the temperature sensitive parameters are separated from the unknowns. Rescaling with δ as the unit of length gives the interesting, but unusable, nondimensional form $Z' = Ra_c(r')^2$.

2.4. *Effects of applied and environmental temperatures*

The utility of the range equation depends upon the extent to which G is independent of the applied temperature $\Delta T/2$ and the environmental temperature T.

Elder's isothermals indicate that the thermal consists mainly of fluid from the leading edge of the boundary layer, which could imply independence of ΔT. But the strongest evidence is that all observers, Sparrow *et al.* in particular, find that increased heat leads to more thermals without changing their nature. This can be readily checked analytically.

Thermal rate

$$N = \frac{1}{\delta^2 t^*} \text{ per unit area in unit time}$$

where

t^* = time for front to reach δ,

$$\text{where } \delta = \sqrt{(\pi K t^*)} \quad t^* \propto \delta^2.$$

From Ra_c:

$$\delta^3 \Delta T = \text{constant}$$

$$\delta \propto (\Delta T)^{-1/3}$$

Hence

$$N \propto 1/\delta^4 \propto [\Delta T]^{4/3}$$

Heat flux

$$H \propto \Delta T/\delta \propto [\Delta T]^{4/3}$$

$$N \propto H.$$

It is perhaps more speculative that G might be independent of environmental temperature. If so, then over the temperature range 20–80°C, K is nearly constant, α increases by a factor of just over 3 whilst ν decreases by just under 3, giving an overall increase in Z by a factor of 9. This was checked with more experimental data as follows.

2.5. *Range measurements for axisymmetric thermals*

The range equation was calibrated using Azhari's data for the range at which his lower convecting zone began to grow, that is, $Z = 44$ cm at $T = 17$°C. Figure 5 shows the resulting graph of Z vs T, on the assumption that G is independent of T and $\Delta T/2$.

Further range measurements were made in a variety of glass and transparent plastic cylinders up to 10 cm in diameter, filled with water at the required temperatures. A diluted food dye was injected with a fine plastic tube and a syringe onto the base, with minimum disturbance. The base was then heated with warm air. Figure 6 shows the kind of axisymmetric thermals seen at short ranges using chilled water, the continuing connection with the source being very clear. At longer ranges for higher water temperatures they tended to wander and the dye became tenuous.

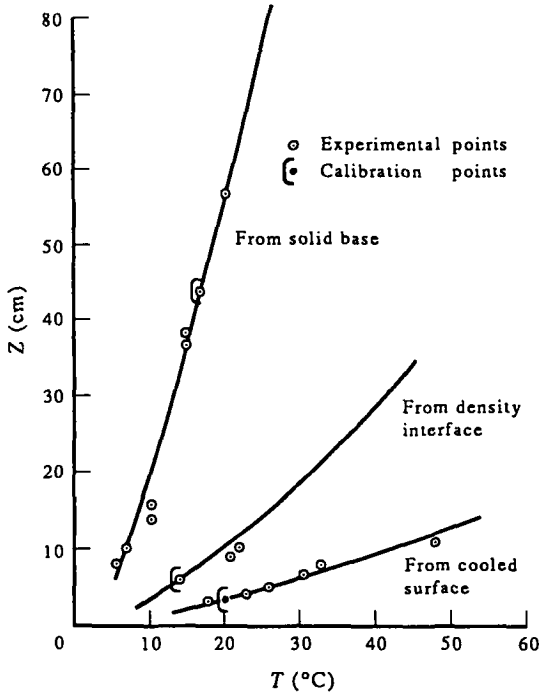

FIG. 5. Thermal range vs environmental temperature.

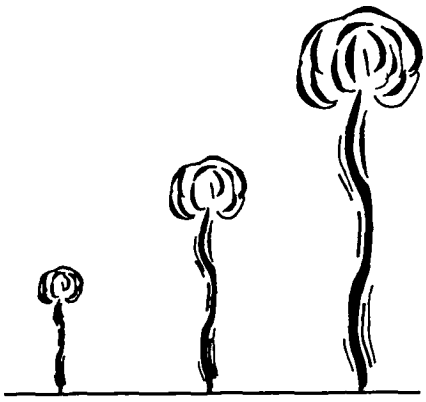

FIG. 6. Axisymmetric thermals.

Nevertheless, the thermal fluid was easily recognised by its considerable and roughly constant velocity of the order of 0.5–1 cm s^{-1}, and by its coming quite abruptly to rest. The scatter in range was about 10% at each value of T. The good fit to the calibration curve shows that G is markedly, if not entirely independent of environmental temperature.

The value of G was 36.1×10^{-12} (in SI units), from which can be derived the orders of δ and r for any given environmental and applied temperatures. δ might be expected to bear some relationship to the initial size of the blob of heated fluid, with r being more an effective value giving some measure (by its smallness) of the effectiveness of viscous damping. For $T = 20$°C and $\Delta T/2 = 1$°C, the boundary layer thickness is 4.29 mm. Hence $r = 1.40$ mm, which is of the order expected.

The independence of range to $\Delta T/2$ was directly checked by immersing the base of a cylindrical vessel in a water bath at a range of temperatures. $\Delta T/2$ in the fluid was calibrated to zero for no thermals. From 0 to 14°C, from no thermals to a rush of many thermals, the range increased by a factor of only 1.2 as shown in Fig. 7. Hence for practical purposes it can be taken that G is a constant, and for axisymmetric thermals:

$$Z = g\frac{\alpha}{K\nu} \cdot 36.1 \times 10^{-12}. \qquad (3)$$

This range equation works remarkably well as regards variation with ambient temperature considering the simplicity of its derivation. To correctly reproduce the roughly constant velocity followed by an *abrupt* stop would require a fresh, more sophisticated approach, taking into account that δ and r are also functions of time. Similarity solutions should be tried. The treatment by Griffiths [18] of thermals and plumes in *very* viscous fluids is of some interest though not directly relevant. The thermals and plumes are *laminar* as in the earth's mantle, and not *turbulent* as in water. They

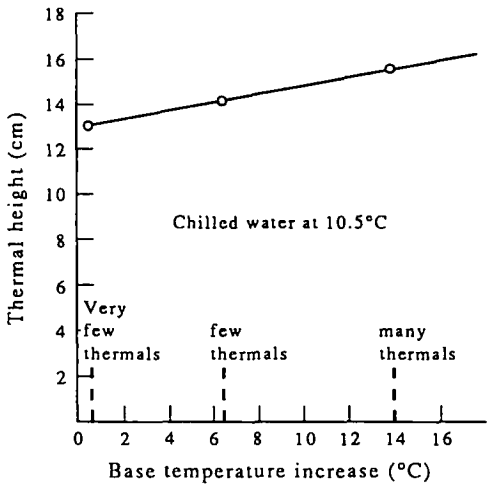

FIG. 7. Thermal range and base temperature.

entrain background fluid by heating it in a boundary layer, rather than through turbulent eddies. Similarity solutions are found and simulated thermals show expanding Hill's spherical vortices. A simulated starting plume looks remarkably like the axisymmetric thermals observed in chilled water.

2.6. *Implications*

Tyical starting conditions for an actual solar pond might be a lower convecting zone of depth 1.0 m at a temperature of 20°C. Solar energy absorbed in the fluid would slowly increase temperatures throughout, but that reaching the bottom, usually a black plastic liner, would produce axisymmetric thermals having an initial range of only 56 cm. The temperature of the lower region, up to the range of the thermals, would increase until the thermals eventually reached the boundary with the gradient zone, as determined by the range equation. Thereafter, the lower convecting zone would grow due to mixing and erosion, producing a salt step. The effect of salt diffusion is, however, to tend to smooth the step. These opposing factors usually result in growth of the lower convecting zone in the summer and decay during the winter. Hence the phenomenon is not a disastrous one. Any attempt to suppress the thermals would upset this balance.

To complete the information on thermals and their effect, further experimental data are required on the amount of heat transported by each thermal and the rate of zone growth in response to a given flux. As regards the latter, work by Azhari [11] already mentioned is relevant.

Although not directly applicable, it is of interest that the effects of thermals were simulated as early as 1961, in an attempt to describe convection processes in the atmosphere. According to Turner [19]:

"Experimental investigations have been made by Richards [7] and Saunders [20] of the conditions under which buoyant thermals can penetrate an interface between two fluid layers of different densities. When the buoyancy is reversed in the second layer, so that the thermal penetrates some distance and then falls back, the phenomena of erosion and wave generation are prominent. These results have been used by Saunders to interpret observations of the growth of large clouds through the tropopause".

The experiments were carried out in glass vessels of about 1 m cube, with water at the top and salt solution below. Artificial axisymmetric thermals were created by overturning a hemisphere containing about 0.5 l of coloured salt solution at the water surface. The behaviour of the thermals was followed photographically, with the degree of penetration of the boundary being varied by the relative densities. Richards was also able to locate the final disposition of the thermal fluid by using cobalt chloride for the first stage of viewing. Residual cobalt chloride ions could then be chemically treated so as to absorb blue light proportional to concentration. Furthermore, Richards observed that if the hemisphere was not rapidly overturned, the motion was more plume-like than thermal, somewhat as observed with real axisymmetric thermals. It should be noted that the development of the thermals as such may differ somewhat from those of concern in this paper in that the buoyancy is chemical not thermal.

3. GROWTH OF AN UPPER CONVECTING ZONE

3.1. *Model observations*

In virtually all temperature and density plots of laboratory models of salt gradient solar ponds, for example those of Fig. 2, an upper convecting zone appears as soon as the surface temperature rises above ambient air temperature. Tsilingiris [6] found that growth persisted long after his solar lamp was switched off. Azhari [11] confirmed these experimental findings without adding anything relevant to the cause.

By analogy with the role of thermals from a heated base, it seemed likely that a surface cooled by evaporation should equally well produce downward thermals with definite range. These would erode the top of the gradient zone and lead to a growing convecting zone. To remove surface heat produced by the infrared radiation from his solar lamp, Tsilingiris used a cooling fan and, from time to time, flushed the surface with cool water. Both would stimulate more downward thermals.

3.2. *Information from the literature*

A literature search was made for observations of fluid falling from a surface cooled by evaporation, and, assuming the same thermal formation mechan-

ism, a critical Rayleigh number for a layer of fluid bounded on one side by air and on the other by a change in fluid density.

Katsaros *et al.* [21] refer to a number of writers from Woodcock [22] onwards, having noted or studied the existence of a cool boundary layer on the surface of natural water bodies due to net upward heat flux. They themselves made extensive measurements of temperature distribution in such boundary layers. For the observation of thermals they refer to work by Spangenberg and Rowland [23], and for the initiation of free surface instability to Pearson [24].

Spangenberg and Rowland used a Schlieren photographic system looking at the open top and one longer side of a glass vessel filled with water to a depth of 10 cm. On removing a plastic cover, they observed that "Streamers of liquid then plunged precipitously from the cooled surface layer. Upon reaching the container bottom...". Runs were carried out at water temperatures of 27.8, 29.5 and 39.2°C in still air. The main effect of greater evaporative cooling at higher water temperature was found to be a greater rate of thermal formation. The Schlieren photographs of the surface showed very clearly the changing pattern of lines from which fell the sheets of fluid. The side views, however, showed a mass of detail of every change in density.

The convergence of water along surface lines is generally attributed to variation of surface tension with temperature. Under appropriate conditions, regular patterns are seen, notably the hexagonal form of Bénard cells which were observed in a shallow dish open to the air at the top. The Marangoni number is

$$M = -\frac{\partial \gamma}{\partial T} \cdot \frac{\partial T}{\partial z} \cdot d^2 \cdot (\rho \nu K)^{-1} \qquad (4)$$

where γ is the surface tension and d the fluid depth. Pearson found that marginal stability occurred at a critical value of $M = 80$, and that the Rayleigh number for the boundary layer was 571. The questions are whether discrete thermals exist, what form they take and what is their range, particularly as a function of environmental temperature.

3.3. *Two-dimensional thermals and range measurements*

Experimental observations were made in a thin walled glass cylinder 8.5 cm in diameter and 14 cm deep, filled with water at 18°C. A diluted food colour was applied to the surface so that it might be entrained with the thermals and show their shape and development. However, the slightest vertical momentum sent the dye to the bottom as spurious thermals, often axisymmetric. Use of a thin floating diffuser 1 cm square improved the situation, but the dye still tended to fall off the diffuser. The eventually successful technique was to dilute the dye with warmer water, introduce it with the diffuser and leave the dye floating on the surface awaiting cooling. A fan was used to enhance evaporation.

Within a few minutes, quite unmistakable two-dimensional thermals were clearly visible, Fig. 8. The vertical and near vertical lines were end views. In profile, the thermals started out like Gaussian distribution outlines, growing and travelling downwards at a roughly uniform speed of about 2 mm s^{-1}, whilst retaining contact with the line source. (This use of the term Gaussian is not to be confused with the time averaged Gaussian distributions of velocity and temperature *within* turbulent plumes.) They came quite sharply to rest at a depth of (3 ± 0.5) cm in one of two terminal states, a symmetrical mushroom or an asymmetric hook, with a width of about 1.5 cm (making due allowance for magnification by the cylinder of water). It is shown later (Section 4) that when the Gaussian profile has a tilt or shear, the fluid, and hence the dye, concentrates on one side to look like a hook. It would have been valuable to have photographic evidence, but the dye is tenuous and there is no substitute for visual observation of the dynamic behaviour. Spangenberg and Rowland did not recognise the two-dimensional thermals, perhaps because of their snap shots in time as compared with continuous viewing by eye (they had tried using dye, without success). Yet knowing now what to look for, Gaussians, mushrooms and hooks can all be identified. Although at their top temperature of 39.2°C the true thermals may have reached the bottom of the vessel, they should not have done so at the lower temperatures. This is confirmed by the presence of the two end states.

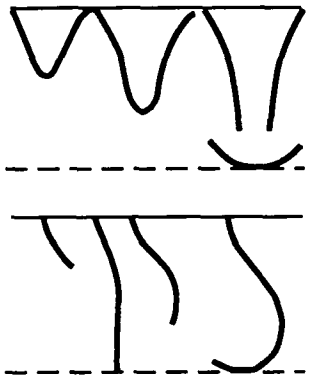

FIG. 8. Falling thermals from a surface to air at various stages of development.

Range measurements were made at temperatures up to 48°C. The range equation was calibrated at 20°C and, as shown in Fig. 5, the further experimental ranges were a good fit to the curve, That the same range equation is likely to fit, can be seen by going back to the form with separate thermal volume V and area A. For near two-dimensional thermals from *cylindrical* blobs of fluid of cross section δ and length l, $V = \delta^2 l$ and $A = \delta l$. Hence V^2/A^2 is again equal to δ^2, independent of l. The lower velocity and much

shorter range for a given temperature are the result of greater area and viscous drag for a given volume. The value of G was 2.36×10^{-12}. For water at 20°C and $\Delta T/2 = 1$°C, $\delta = 3.44$ mm and $r = 0.45$ mm, as compared with $\delta = 4.29$ mm and $r = 1.40$ mm for axisymmetric thermals.

3.4. *Growth of a convecting zone*

Having established the existence of discrete thermals with definite ranges, their role in establishing an upper convecting zone could then be examined.

A plastic vessel 15 cm across was filled with a 5% salt solution at the ambient air temperature of 17°C, to within 1.6 cm of the top. A 1.5 cm layer of plain water also at 17°C, in which the thermal range would be 2.5 ± 0.5 cm, was very carefully diffused onto the top using a small cork mat. Dye was added to the surface at the edge of the container with further dye at the centre.

Evaporation was enhanced by a fan blowing across the surface. Within 5 min a well defined line of dye extended right round the interface, marking it very clearly. As shown in Fig. 9, growth of the upper zone began virtually immediately and was linear up to about 7 h. It then slowly levelled off to 2.8 cm after 30 h. The upper water temperature fell slowly to 15°C.

The slow approach to a limiting depth reflected the scatter in thermal range. The ultimate limit of 2.8 cm was the maximum depth of falling thermals at 16°C, that is, $2.3 + 0.5 = 2.8$ cm. The centrally introduced dye took about 3/4 h to be stirred into a uniform colouration. Hence, whilst the thermals immediately eroded the boundary, they took a considerable time to stimulate convective circulation.

3.5. *Implications*

There is immediate relevance to the behaviour of solar pond models in the laboratory. Evaporation is enhanced by heat from the base diffusing through to the top and raising the temperature above that of the ambient air. An upper convecting zone grows, and continues to grow after the heat source is switched off.

When solar ponds in the field grow an upper convecting zone it is usually attributable to wind induced waves and mechanical mixing. Floating plastic nets or rings are used for suppression. However, it seems very likely that thermals can be responsible in some cases since evaporation is necessary to get rid of surface heat—that due to infrared radiation and that conducted through the gradient zone. Wind would play a supporting role by enhancing evaporation. Such an upper convecting zone seems the more likely in those geographic areas having the best insolation conditions since they tend to have high ambient temperatures and, on occasions, strong winds.

It is highly questionable whether any attempt should be made to prevent falling thermals. With a surface temperature of 35°C the thermals would still fall no more than 10 cm, with this being the limiting depth of the resultant convecting zone. The loss in pond efficiency would not be serious. Suppressing the thermals by using a thin film of oil or plastic on the surface would have dire consequences. With the loss of evaporative cooling the whole level of temperatures in the pond would rise with catastrophic results.

4. BREAKDOWN OF THE GRADIENT ZONE

4.1. *Observations and criteria*

Early thinking on this matter was much influenced by the pioneering work of Turner [8, 9] on double-diffusive convection. Theoretically and experimentally, he showed how in water with a uniform gradient of salt 'strongly' heated from below a lower convecting zone would grow continuously for a time, followed by emergence at the top of this zone of a *succession* of new convecting zones. Further analytical and experimental work was carried out by Huppert and Linden [25] applying power levels of 420–4200 W m^{-2} at the base. Essentially Turner's rate of heating was such that the vast majority of the heat had no

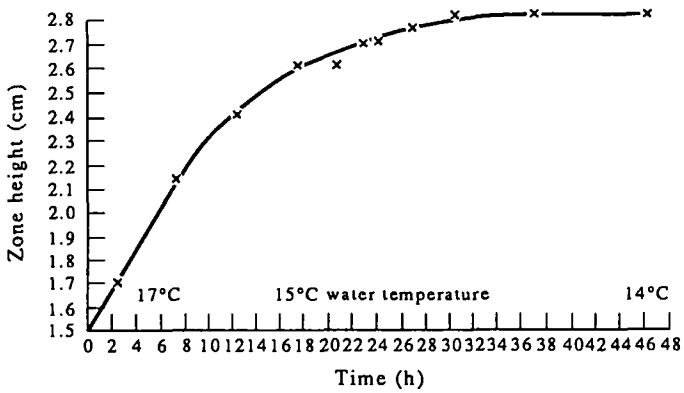

FIG. 9. Upper convecting zone height vs time—at final temperature of 14°C.

time to diffuse beyond the convecting zone, but when some eventually did so, the temperature gradient was so large as to produce overturning and a rapid succession of new zones. Huppert and Linden gave it among their own and Turner's assumptions that the heat of the thermal boundary layer ahead of the advancing front could be neglected in calculating the heat budget for the layers and that the density step was zero.

As already seen, these conditions are certainly not the case in solar pond models heated wholly or mainly at the base *with the equivalent power of solar radiation*, which, at its very best, has a daily mean value of only 300 W m^{-2}. Accordingly, Tsilingiris [6], using a solar simulation lamp and the models, equipment and techniques described in 2.1, was unable to reproduce *successive* new zones. Yet Azhari [11] was able to do so by raising his electrical heating at the base far beyond that used in his own experiments. The evidence was conclusive that the Turner/Huppert and Linden model does not apply to any system, natural or artificial, where the heating is solar or of solar magnitude. An alternative was needed.

Eventually Tsilingiris found that it was necessary to reduce the maximum salt concentration at the bottom to 10% or less, and to continue heating for several days, in order to induce breakdown of the gradient zone. His short time interval between scans (a few minutes) showed conclusively that a number of new convecting zones appeared *simultaneously not successively*. A range of experimental runs was made with different parameters to observe the conditions at which instability occurred.

Subsequently, Tsilingiris [6] and Tsilingiris and Mullett [10] showed that there was a very good fit of these data to a dynamic stability criterion first published by Weinberger [4], [26]:

$$\frac{ds}{dz} \geqslant -\frac{\nu+K_T}{\nu+K_s}\cdot\frac{(\partial\rho/\partial T)_s}{(\partial\rho/\partial s)_T}\cdot\frac{dT}{dz}$$

where s is the salinity and K_T and K_s are the diffusivities of heat and salt. Since K_s is very much smaller than K_T

$$\frac{ds}{dz} \geqslant -\left(1+\frac{K_T}{\nu}\right)\cdot\frac{(\partial\rho/\partial T)_s}{(\partial\rho/\partial s)_T}\cdot\frac{dT}{dz}. \qquad (5)$$

The salt gradient for dynamic stability $(ds/dz)_{dyn}$ has to be greater by a factor of $(1+K_T/\nu)$ than that for static stability $(ds/dz)_{stat}$. The factor is usually quoted as 1.14, but this is its value at 20°C. The maximum base temperature of a solar pond is of the order of 80°C, at which the factor needs to be 1.40.

Figure 10 shows the outcome of the most carefully contrived run for a maximum salt density of 4.9%, with a near-uniform temperature gradient over the gradient zone at breakdown. As usual, the details were best seen in the temperature scans, and in that marked ×——× there were seven new zones. Their heights averaged 1.34 cm, and the temperature difference across each of the five inner zones was 2.3°C, giving Rayleigh numbers of 1.7×10^5. The uppermost of the new zones had a much higher temperature difference of 11°C from the upper convecting zone, giving a cell total of 12°C and a Rayleigh number of 9×10^5. The lowest of the new zones had 9°C to the lower convecting zone, giving a cell total of 10°C and $Ra = 7.5\times10^5$. The replacement of conduction throughout the gradient zone by such large measures of convection with conduction in between led to a far greater rate of heat transfer to the surface. The rise in top temperature was so marked that the difference in density between top and bottom, which had been falling, rose again.

In earlier scans, all that could be seen was the almost simultaneous emergence of these seven, high Rayleigh number zones, without the preliminary of a larger number of zones with lesser Rayleigh numbers. In later scans, the new zones merged until only three were left when the run was prematurely terminated by a leak in the tank. Other runs taken to completion showed that the new zones eventually merged into one, and, finally, the whole tank convected from top to bottom.

It is not known how Weinberger derived his criterion since the earlier 1962 paper [26] was an internal publication not generally available. The 1964 paper [4] concerning solar ponds, describes the condition as that required to prevent oscillatory motion growing with time. The most obvious starting mode is the Brunt–Väisälä buoyancy oscillation. If the density gradient is vertical and uniform, vertically displaced fluid is subject to a central restoring force and the resulting angular frequency is

$$N = \sqrt{(g/\rho\cdot d\rho/dz)}.$$

Viscous forces damp out perturbations provided that this frequency is sufficiently high.

At the point of instability the part density gradient due to salt $(ds/dz)_{stat}\cdot(\partial\rho/\partial s)$ is cancelled out by the density gradient due to temperature, leaving

$$\frac{d\rho}{dz} = -\frac{K_T}{\nu}\left(\frac{ds}{dz}\right)_{stat}\cdot\frac{\partial\rho}{\partial s}.$$

In terms of the starting gradient $(ds/dz)_{dyn}$

$$N = \sqrt{\left[g/\rho\cdot\left(\frac{ds}{dz}\right)_{dyn}\cdot\frac{\partial\rho}{\partial s}\cdot\frac{K_T}{\nu+K_T}\right]}. \qquad (6)$$

At temperature gradients beyond critical, the frequency is too low for viscous damping to be effective and oscillations grow exponentially in amplitude.

Veronis [27], also considering a density gradient, was principally interested in the possibility of finite amplitude transition to instability, but he first derived a stability criterion for the small amplitude transition to an overstable (oscillatory) mode with horizontal wave number α and vertical wave number n. As with Weinberger, the oscillation began to grow before the

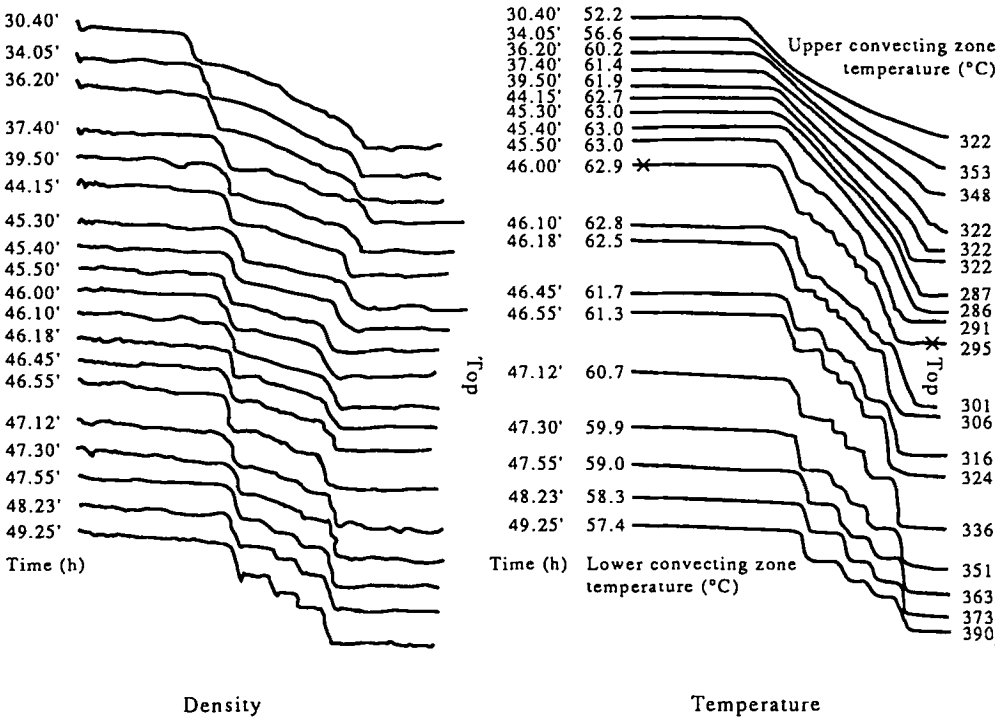

FIG. 10. Density and temperature profiles in a solar pond model (Tsilingiris [6]).

static limit was reached, and an increase in salt gradient of $(1+K_T/\nu)$ was required for stability, leading to the same stability criterion (equation (5)). The angular frequency p_m in dimensionless form was given by:

$$p_m^2 = \frac{\sigma\alpha^2}{(1+\sigma)(\alpha^2+n^2)} \cdot R_s$$

where $\sigma = \nu/K_T$, that is, the Prandtl number, and R_s is the salinity Rayleigh number. If α is very large, the overstable mode reduces to buoyancy oscillation with frequency given by

$$p_m^2 = \frac{\sigma}{1+\sigma} \cdot R_s.$$

As expected for linear (small amplitude) oscillations, this is independent of n, and when converted to dimensional form it is identical to that obtained from Weinberger's criterion (equation (6)). The argument is a circular one, but it is a satisfying check on algebra.

Clearly, with this criterion it no longer matters whether the solar pond is shallow with the bulk of the heat being released at the base, or deep with a proportion of the heat contributing directly to the temperature gradient. Moreover, it applies also to the widely occurring density layers in the oceans where *all* the solar radiation contributes directly to the temperature gradient. By contrast, although Turner, Huppert and Linden, and Fernando [28] all mention this case as possibly related to their model, it cannot be so.

It remains to determine how the layers originate physically. Tritton [29] also considers that instability starts from buoyancy oscillations and overstability at low Rayleigh numbers, but cannot offer an explanation of how actual systems proceed to zones of high Rayleigh number. Since the Tsilingiris scans show no sign of new zones at lower Rayleigh numbers, it seems that there must be finite amplitude transition from buoyancy oscillation to convection at Rayleigh numbers $>10^5$. A Rayleigh number of 10^5 implies turbulence and, as will be shown later, a number of this order also means the onset of heat transfer by thermals. The first question is whether such thermals exist, and, if they do, what form they take.

There are somewhat vague references in the literature to fluid rising and falling from a density boundary, and Linden and Shirtcliffe [30] use such a model for a double-diffusive interface. Thermals are considered to rise and fall from boundary layers on either side which become unstable by the Howard mechanism. They were not able to offer any specific kind of thermals other than the axisymmetric form of Sparrow *et al.* which is relevant only to a solid surface.

4.2. *Thermals from a density interface*

The boundaries between the new zones after breakdown are substantial steps in density due both to temperature and salt discontinuities. They are of the 'free surface' kind considered by Rayleigh [31]. The effective extent of each boundary layer, upwards and

downwards, can again be defined by the advance of complementary error functions in temperature and time (equation (1)). Each boundary layer at emission of thermals would then have a critical Rayleigh number as first calculated by Rayleigh for two 'free' surfaces, namely $27(\pi^4/4) = 657$.

As early as 1883, Rayleigh [32] had considered the somewhat similar Rayleigh–Taylor problem of a density step due, say, to a temperature difference between a layer of cooler water over a layer of warm water. Elder [17] computed what happens to the back-to-back boundary layers in this case. He used a critical Rayleigh number of 650. Figure 11 shows the isothermals with buoyant thermals ready to emerge, both upwards and downwards.

From the Rayleigh number of 657 for instability, the thermal range for a given temperature was anticipated to be somewhat greater than from a cooled surface (with $Ra_c = 571$) but still much less than from a heated solid base (with $Ra_c = 1101$). Experimental observations were carried out in a transparent plastic cylinder 10 cm in diameter, with a height of 20 cm. The cylinder was half filled with a 5% salt solution at an initial temperature of 30°C. A thin cork diffuser was placed on the surface and the whole allowed to settle. The top half was filled with water at 14°C by pouring slowly onto the diffuser, using extreme care, especially to begin with. Any fluid allowed to fall onto the surface immediately plunged downwards and damaged the interface, which could be seen by reflection and refraction. A syringe with a thin plastic tube extension was filled with food dye diluted with water at 14°C. Again with extreme care, the tube was inserted at a steep angle to the interface and about 3 mm above its centre. A blob of dye was placed on the boundary layer and the tube carefully removed.

Almost immediately, upward thermals were seen which were very clearly two-dimensional with Gaussian-like profiles. However, the Gaussians were all tilted to one side as shown in the top half of Fig. 12. The tilt or shear was generally in the direction of withdrawal of the plastic tube, and may have been so imparted. Not only were the outlines more clearly visible than in the case of thermals from a cooled surface, but the flow of fluid within the thermals could be clearly seen as continuing from the base towards the direction of shear of the Gaussians. The end states all appeared as hooks. There were no upright Gaussian profiles and, hence, no mushroom end states. (The mushrooms and hooks from a surface cooled by air are confirmed to be simply different end states of basically the same phenomenon.) The most obvious reason for the thermals to be two-dimensional is that Marangoni effects occur at the interface. Surface tension is affected by temperature and salt concentration, although there is the complication that the changes are in opposite directions. It increases with more salt but decreases with higher temperature. The best evidence available is from Linden and Shirtcliffe [30] who obtained a shadowgraph plan view of a sugar/salt diffusive interface which shows a mass of 'collective instabilities'. Besides straight lines, there are clear signs of hexagons.

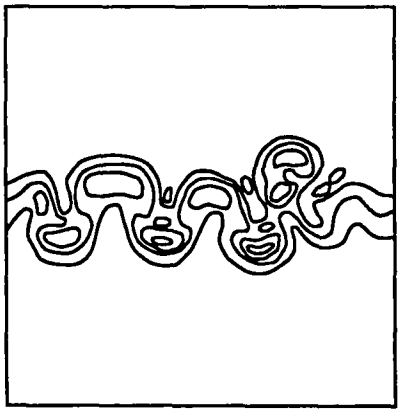

FIG. 11. Growth of thermals upwards and downwards from a density interface (Elder [17]).

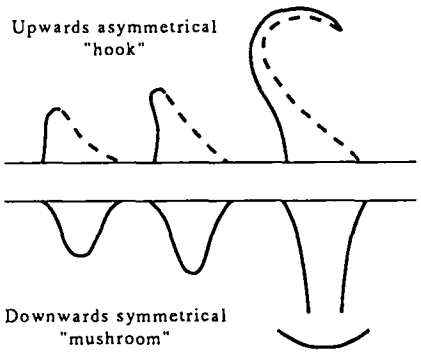

FIG. 12. Gaussian two-dimensional thermals from a density interface.

Figure 5 shows the range/temperature relationship (equation (2)) calibrated with these data. The value of G was 7.30×10^{-12}. At $T = 20$°C and $\Delta T/2 = 1$°C, the boundary layer thickness for $Ra_c = 657$ is 3.60 mm. Hence $r = 0.75$ mm, and is of the order expected for two-dimensional thermals with a somewhat greater range than those from a cooled surface.

It was noted occasionally that dye remained trapped in the boundary layer, yet further dye placed *on* the boundary layer showed the continuing presence of thermals. Something similar had been seen in looking at thermals from a heated base and from a cooled surface, but it was not checked that thermals were still present. This could be a practical illustration that the liquid in the thermals comes mainly from the leading edge of the boundary layer.

Obtaining further data at higher temperatures was much more difficult. Fluid on both sides of the bound-

ary had to be at elevated temperatures. Mixing during filling was more difficult to avoid, even with a 10% salt solution or a 20% sugar solution (which clears more quickly). Furthermore, the interface was more sensitive to perturbation by the dye injection probe and the dye itself. However, two further points were eventually obtained, 9.25 cm at 21°C and 10.5 cm at 22°C. Bearing in mind the difficulties, they were satisfyingly close to the calibration curve. Clearly a more sophisticated diffusion system is required for filling, together with a non-interactive method of observation of thermals, such as the Schlieren photography of Spangenberg and Rowland [23] or the electro-chemical technique of Sparrow *et al.* [14].

Attempts to view and measure the downward thermals met with no success. The plastic tube from the syringe had to penetrate the boundary layer, with inevitable disturbance. But the insuperable problem was that the dye needed to be diluted with salt solution at just the right temperature to rest against the underside of the boundary layer. Although the occasional sign of a thermal was seen, in the main the dye either rose permanently into the boundary layer or fell to the bottom. A non-interactive method of observation of thermals is essential. Nevertheless, there is no reason to doubt the presence of downward thermals with the same range/temperature relationship. As with thermals falling from a cooled surface to air, it can be expected that at least a proportion of the Gaussian profiles would fall symmetrically and terminate as mushrooms, as indicated in the lower half of Fig. 12.

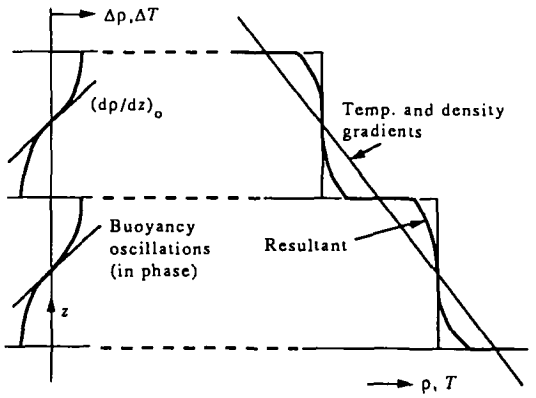

FIG. 13. Schematic effect of a critical amplitude of buoyancy oscillation on the gradient zone.

4.3. *The roles of thermals*

It can now be considered whether such thermals play a part in direct transition from buoyancy oscillation to high Rayleigh number convection zones. The transition might begin with buoyancy oscillations consisting of a number of horizontal density bands vibrating vertically in phase, with growing amplitude. Figure 13 illustrates such oscillations in temperature and density superimposed on a uniform gradient. A number of temperature and density steps would appear. At a suitable amplitude of the buoyancy oscillations, temperature and density would be uniform over the central region of each step, whilst the ends would look remarkably like the boundary layers of convecting zones. With continued increase in the height of the zones, the 'boundary layers' could become unstable at $Ra_c = 657$. Thermals would then emerge and convection begin directly at the appropriately high Rayleigh numbers. Further theoretical and experimental investigation would aim to confirm that this is the preferred transition rather than the more conventional overstable oscillation.

Whichever the approach to convection, when it had reached the measured Rayleigh numbers in excess of 10^5 there must have been thermals, both upwards and downwards, in each zone. In scan ⟷ of Fig. 10, the highest of the new zones had a top $\Delta T/2$ of 11°C as compared with the average of 1.15°C. Since the rate of thermal formation is proportional to $(\Delta T)^{4.3}$ there were 20-times as many thermals going downwards as upwards. Hence, as is very clearly seen, this zone grew at the expense of the next one down. The lowest of the new zones had a bottom $\Delta T/2$ of 9°C, giving 18-times as many upward thermals as those coming downwards. The lowest zone absorbed the next zone above. The process continued, with the top and bottom of the new zones absorbing the rest until only three were left. Had the run not been terminated, the process would have continued until only one zone was left.

Although there are many details left to investigate, there seems no doubt that the Tsilingiris and Mullett model of double-diffusive convection, based on Weinburger/Veronis, is appropriate for solar powered systems, and that the specifically identified buoyant thermals play causal roles in all the physical phenomena. Furthermore, these same thermals provide the physical mechanisms for the Turner/Huppert and Linden model at much higher power levels. Their rapid growth of the lower convecting zone must be due to a copious supply of axisymmetric thermals from the 'strongly' heat base, whilst the eventual short sharp temperature gradient in the salt gradient zone is overturned by upward two-dimensional thermals. Huppert and Linden [25] say "Merging (of zones) produced by the mean vertical migration of an interface is not yet understood and is not included in our model". Again the relative fluxes of upwards and downwards two-dimensional thermals must have been responsible. Fernando [28], also working in the 'strong' region at 700–4500 W m^{-2} realised this need for physical mechanisms and made shadowgraphs in a vertical plane of the lower convecting zone and the emerging zones above. However, this technique, like Schlieren photography, shows such a mass of detail that Fernando was able only to distinguish 'eddies' rather than the individual thermals.

5. CONVECTION BY THERMALS

5.1. *Heat transfer by thermals*

Table 1 summarises data concerning the three classes of thermals from the three possible kinds of boundary. Much has been said about their special roles in double-diffusion and in solar ponds. However, little has been said concerning the general role of thermals in the process of convection and the order of vertical dimensions at which classical convection becomes 'turbulent' and heat transfer by thermals takes over. From then onwards, each horizontal convecting layer has *two* sets of buoyant thermals, upwards and downwards, with the type and range being determined by the nature of each boundary.

Heat supplied at the lower boundary is transported by conduction within the boundary layer, and then beyond it as heated fluid quantised according to the thermals appropriate to the boundary. The fluid transported upwards by thermals is replaced by cooler fluid drawn into the boundary layer. If the rising thermals have sufficient range, determined by their type and the environmental temperature, they are stopped by the density change at the leading edge of the upper boundary layer. Fluid from the upper boundary layer, cooled by upward conduction of heat or by evaporation, is transported downwards as appropriate thermals with corresponding range. Heated fluid, the debris of upward thermals, is drawn into the upper boundary layer as replacement. The falling thermals go as far as they can, and the cycle then repeats. The resultant circulation and mixing is seen in all the thermal experiments using dye, as eventual uniform coloration. Tritton [29] also outlines this process but without the specificity of this new knowledge of thermals.

If the range of the upward thermals from a heated base is less than the vertical height of the cell, the fluid up to that distance becomes heated until, eventually, the range does extend to the vertical height. It seems remarkably fortuitous for practical systems that the range of axisymmetric thermals from a heated solid base is so great. Relevant design data can be obtained directly from the range equation for axisymmetric thermals as a function of environmental temperature. Equivalent Rayleigh numbers for the cell would cover a very wide spectrum, depending also on the applied temperature difference. Downward thermals, unless also from a solid top, have much shorter ranges such that the cooling due to the upper boundary is more confined. Equivalent Rayleigh numbers would cover a quite different range. Again Tritton [29] described this phenomenon, but as occurring when "...at the highest Rayleigh numbers, the thermals lose their identity...".

5.2. *Salt gradient solar ponds*

A full size salt gradient pond operates throughout according to this mode of convection by thermals, both normally and should the gradient zone break down into further convecting zones. This is also true at the typical scale of laboratory models. Figure 14 shows schematically how each convecting zone has two sets of thermals. Except for the already known axisymmetric thermals from the base, all the rest are 'two-dimensional Gaussian', including those upwards and downwards from the top and bottom of the gradient zone. Their roles have been described. Little specific data are available from solar pond literature. Hull and Mehta [33] in looking at a possible model of gradient zone erosion, refer to a number of papers by other authors on flow visualisation in the lower convecting zone. It is there noted that "Fluid flow in the bottom convecting zone is characterised by mildly turbulent convection, consisting of thermals rising from the heated bottom and descending from the gradient zone boundary".

There are three unknowns left to investigate. The first concerns the quanta of fluid and of heat in each of the three types of thermals. The boundary layer thickness is involved in determining volume, but this is itself a function of applied temperature difference in such a way as to suggest that it is the amount of heat which is principally quantised. Optical counts of thermals against time at a variety of environmental and applied temperatures would resolve the matter. The electrochemical technique used by Sparrow *et al.* seems well suited to continuous visualisation and counting of thermals.

Still less is known, as yet, about the quantification of boundary mixing and erosion. The density steps are such that impacting thermals are turned around with extremely small penetration, but the cumulative effect of many thermals is large. Laboratory experiments using a simple density step would provide basic data from which to determine what happens in actual systems such as solar ponds, but there are many vari-

Table 1

Boundary layer	Ra_c	G $\times 10^{-12}$	Range at 20°C [m]	δ [mm]	r [mm]
Solid–liquid	1101	36.1	0.565	4.29	1.40
Liquid–liquid	657	7.30	0.105	3.60	0.75
Liquid–air	571	2.36	0.033	3.44	0.45

For $\Delta T/2 = 1$°C

Range $= g(\alpha/K\nu)\cdot G \quad G = \delta^2 r^2 \Delta T/2$
$Ra_c = g(\alpha/K\nu)\cdot \delta^3 \Delta T/2.$

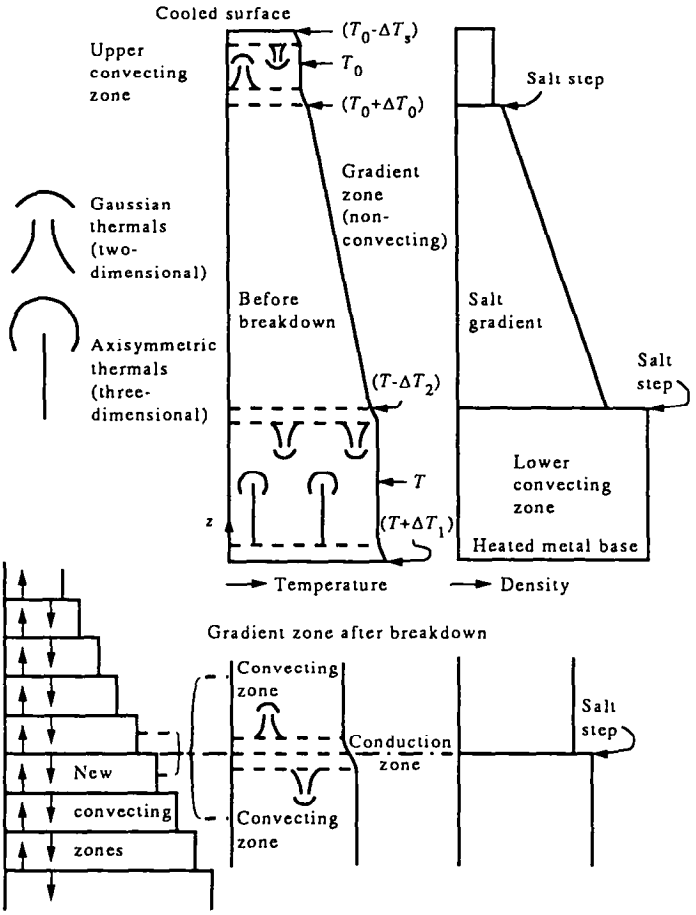

FIG. 14. Schematic of thermals in a salt gradient solar pond.

ables which could be significant. From the model experiments of Azhari [11] it is already known that the size of the density step at the impacted boundary is a variable. Fortunately, it seems that thermal velocity is not a significant function of thermal height (until the thermals come sharply to rest) so that some simplification might be possible. Given the results of thermal quantisation experiments, it would not be necessary to observe and count the thermals. Their flux could be computed from power input.

Finally, what happens when the impacted boundary is that of the gradient zone in an actual solar pond depends upon the extent to which a density step develops during the thermal build-up of the pond. There is need for accurate measurements in the field using a temperature/density scanner of the Tsilingiris type.

5.3. *Thermals in relationship to turbulence*

Generally it is believed that turbulence replaces laminar flow at Rayleigh numbers of the order 10^5, although according to Rossby [34] it occurs at $Ra \approx 14\,000 Pr^2$, where Pr is the Prandtl number and $\alpha = 0.6$ for $Pr \gg 1$. For water at 20°C, $Pr \approx 7$, so that $Ra = 45\,000$. However, knowledge of the origin of thermals enables a more explicit view to be taken.

Figure 15 shows diagrammatically how convection by thermals should develop for the particular case of two horizontal solid surfaces. The vertical parameter is $M = d/\delta$ where d is the cell height and δ the critical boundary layer thickness for thermal emission. The temperature distributions are schematic.

First is shown the lower boundary layer for an infinitely deep cell. The temperature distribution starts as a complementary error function, $\operatorname{erfc}(z/2\cdot\sqrt{(K\cdot t)})$, with $\Delta T/2$ as the applied temperature difference at the base. The tangent to the complementary error function at $M = 0$, shown as a broken line, determines the effective critical depth of the boundary layer at $M = 1$. The thermal, ready to emerge, is shown as a circle of diameter $M = 1$. In three dimensions it would be a sphere for an axisymmetric thermal. The upper surface of the boundary layer is taken to be of the 'free' surface, density difference type. The critical number for thermal emission is $Ra_c = 1100$. Hence, in terms of the nondimensional height M, all Rayleigh numbers for complete cells with total applied temperature ΔT, are:

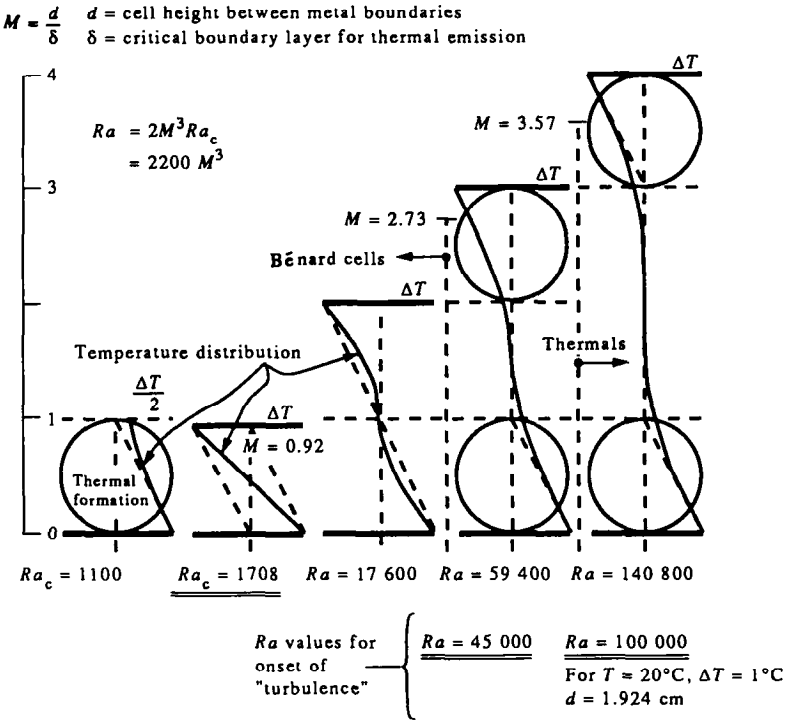

FIG. 15. Schematic of transition from Bénard–Rayleigh convection to convection by thermals.

$$Ra = 2M^3 \cdot Ra_c = 2200M^3,$$

independent of T and ΔT.

Next is shown the complete cell at which classical convection starts. The critical Rayleigh number is 1708, so that the vertical height is $M = 0.92$. The temperature distribution is linear.

Cells are then shown at integral values of M. For $M = 2$, the boundary layers cannot proceed to thermal instability since T and dT/dz must be continuous at the centre of the cell. Ra is 17 600. The convection is of Bénard/Rayleigh type with instability and fluid flow end to end of the cell.

$M = 3$ is clearly the transition point. It is not immediately obvious whether or not the boundary layers can proceed to instability. If they did so, then the heat transfer would be by thermals emerging from each boundary layer but not having any free flight. Ra is 59 400.

For $M = 4$, there is no doubt that the boundary layers do become unstable with a region of zero temperature in the middle of the cell. The thermals have free flight and provide full heat transfer. Ra is 140 800.

At the turbulence value of $Ra = 45\,000$ due to Rossby, M is 2.73. At the generally accepted value of $Ra = 100\,000$, M is 3.57. The assumption that turbulence means heat transfer by thermals around $M = 3$ seems well founded. This is indicated in Fig. 3 by repeating and inverting Howard's mean temperature distribution so as to make a cell with $M = 3$. Howard's depth parameter ξ is such that $z = \delta$ and $M = 1$ at $\xi = 0.885$. Further evidence can be sought from measurements on complete cells and calculated temperature distributions.

Measured temperature distributions for complete cells are mainly for air and lower Rayleigh numbers. Gille [35], for example, goes as far as $Ra = 2.7 \times 10^4$. However, more significant information is available concerning Nusselt numbers (Nu is the ratio of the actual heat flux to the purely diffusive heat flux with a hypothetical linear gradient of the same overall temperature between the same boundaries).

When the boundary layers are separated, it is found experimentally that $Nu = c\,Ra^{1/3}$, again implying fixed boundary layers, with wider spacings for higher Rayleigh numbers. According to Turner [9], the best values of c are 0.08 for air and 0.09 for water. For air, the initial slope of Howard's curve gives good agreement:

$$Nu = (\Delta T/2\delta)/(\Delta T/d)$$
$$= d/2\delta = 3.061 = 0.078(Ra)^{1/3}.$$

For water, with a complementary error function boundary layer and $Ra_c = 1101$:

$$Nu = \frac{d}{2\delta} = 0.4\left(\frac{Ra}{Ra_c}\right)^{1/3} = 0.038(Ra)^{1/3}.$$

Hence it can no longer be arbitrarily assumed that δ_0 determined by the initial slope is the same as δ_c for criticality of the boundary layer. If $d/2\delta_0$ is to be

$0.09(Ra)^{1/3}$, then $\delta_c = 2.37\delta_0$. Since there is no better assumption for Ra_c, δ_c requires the full extension of the erfc down to 1% of its initial value. The boundary layers then appear more separated, in line with the trend of measured temperature distributions. Howard's distribution for air gives a satisfactory value of Nu since for an appreciable time after the boundary layer has been stripped, the erfc is less advanced. The boundary layer distribution in water may, perhaps, lie between a complementary error function and Howard's average.

Theoretical derivation of temperature distributions, even with spatial means taken over horizontal planes, is notoriously difficult. Herring [36, 37] and Elder [38] used the Boussinesq approximations, suitably non-dimensionalised so that the flow was specified by the Rayleigh and Prandtl numbers. Severe assumptions and simplifications had to be made, prompting Elder to write "The reader unfamiliar with the ruthless approximations needed to cope with turbulent studies may be surprised that the approximations work at all". Nevertheless the results were at least qualitatively correct in that the distributions consisted of two boundary layers, looking much like complementary error functions, well separated and becoming even more so as Rayleigh number was increased.

However, numerically there were problems. Herring [36] for two 'free' boundaries had such narrow boundary layers that Nu was $0.31\ (Ra)^{1/3}$. Herring [37] for two solid boundaries, still had boundary layers somewhat narrower than expected, with Nu being $0.135\ (Ra)^{1/3}$. Elder's results [38] were very similar. The value of Ra_c for the boundary layers was, at the most, 150, needing δ to be larger by about a factor of two for the critical value. However, it is Elder's computational procedure which is particularly interesting. Instead of scaling his equations in terms of cell height d, he used δ, and found that δ could be chosen such that $A\delta^3 = Ac =$ constant. (Throughout his researches, Elder used Rayleigh's original symbol A.) Hence, when the boundary layers were separated, a single solution served for all Rayleigh numbers from somewhere in the range 10^4 to 10^5 upwards. It cannot be said precisely what numerical changes there would have been in Elder's result had he recognised that Ac should have been in terms of the applied temperature $T/2$ not T (in his terminology). But, in dimensional form, his relationship would have been $A = 2\ (d/\delta)^3 Ac$, the exact equivalent of $Ra = 2M^3\ Ra_c$.

It can be concluded that experimental values of Nusselt number and analytical spacial means of temperature over horizontal planes confirm the physical view of heat transfer by thermals which is illustrated in Fig. 15. Instead of laminar flow simply becoming turbulent at $R \sim 10^5$ there is a complete change of mode of heat transfer to the quantised form of thermals. (This can only be detected by visualisation of the thermals since the stochastic nature of the thermals gives temperature fluctuations at a point as in turbulence.) It seems also, at least to a first order, that greater heating (or cooling) rate leads to a proportionally greater rate of thermal quanta.

An almost identical diagram to that of Fig. 15 can be constructed for convection between two 'free' surfaces of the fluid density step type. Ra_c for thermal formation is 657, and so too is Ra for the onset of cellular convection. Since Ra_c is in terms of $\Delta T/2$ and Ra in terms of ΔT, the value of M for the critical cell is 0.79. The rest of the diagram looks the same, with the likely transition at $M = 3$ being at $Ra = 35\,500$. This is the value which should apply to the new convecting zones formed when the gradient zone of a salt gradient pond breaks down.

The diagram is slightly more complicated if the top and bottom surfaces are different, such as a solid vessel open to air. If M is chosen to be unity for the lower boundary layer, then M for the upper boundary layer will be determined by its appropriate Ra_c value in relationship to that for the lower boundary layer. It would seem reasonable to determine the transition point on the basis of the spacing between the boundary layers being equal to the size of the larger thermal. Solar ponds involve two such cases, the solid base to density step and the density step to surface to air.

It is apparent also from the diagrams that classical convection occupies only a small region of spacing between horizontal surfaces from about 0.4 cm to the order of 2 cm. It is clear that the behaviour of a salt gradient solar pond, even at the usual laboratory scale, is entirely characterised by convection by thermals, as must be many other natural and artificial systems.

6. CONCLUDING REMARKS

The principal objective of this work was to shed some light on the fluid mechanics of salt gradient ponds. In retrospect, it is no coincidence that all the questions have been answered, satisfactorily it is believed, in terms of buoyant thermals. When eventually it had been shown that quantised heat transfer by thermals takes over from Bénard–Rayleigh flow at Rayleigh numbers of the order of 5×10^4 to 10^5, it became clear that solar ponds function, and malfunction, in the 'thermal' mode, and, fortunately for it was not planned at the time, so do laboratory models at about 1/6 vertical scale. The lack of much earlier progress was entirely due to the inadequacy for the purpose of the state of knowledge of buoyant thermals at that time.

The existence of axisymmetric thermals from a heated solid base was well known, and their role in heat transfer had been described quite recently. It was much less well known, though quite widely reported in the literature, that near-two-dimensional sheets of fluid fell from an open surface cooled by evaporation, starting from ridges related to surface tension. There were a few vague references to 'mild thermals' from density/temperature interfaces.

From the research reported in this paper, it is now

known that axisymmetric thermals can retain their identity to very considerable distances. The falling sheets from a cooled surface are near-two-dimensional thermals of initially Gaussian profile, terminating in a head which appears as a mushroom or a hook, depending upon whether the Gaussian travels true or with a 'shear'. Density/temperature boundaries also show two-dimensional Gaussian thermals travelling upwards with a 'shear' and terminating in a hook. Although the available experimental technique was not adequate to view them, there is ample evidence, particularly theoretical, that there are downward plumes at the same time. Hence the three possible kinds of boundary each have their characteristic thermals. Whatever the combination of boundaries, a convecting cell has both upwards and downwards thermals providing heat transfer.

All three categories of thermals have distinct ranges which increase markedly with environmental temperature according to a common law but varying in scale. Those from a solid boundary show by far the greatest range, and those from a surface to air the least, all consistent with the Rayleigh instabilities of the boundary layers and the forms of the thermals. There is no heat transfer when the cell height is greater than the appropriate thermal range. The boundary then heats or cools locally, until the range is sufficiently extended. Only the number of thermals, and not the range, is affected by applied temperature (that is, input or output power).

In solar pond models, and in supplementary experiments, all three kinds of thermals show that when their range exceeds the height of the cell, boundary mixing and erosion occurs, that is, they are responsible for 'penetrative convection'.

There is also evidence to suggest that buoyant thermals might be responsible for finite amplitude transition from buoyancy oscillation directly to high Rayleigh number convection.

It follows that for double-diffusive systems generally, the physical phenomena are determined by the presence and the behaviour of buoyant thermals. This applies both to the Tsilingiris and Mullett model which is relevant to solar powered systems, *and* to the Turner/Huppert and Linden model which is relevant only to systems much more strongly heated at the base.

These were the missing links in explaining the behaviour of salt gradient solar ponds. They must be relevant also to other natural and artificial systems of sufficient size, and could be equally illuminating.

Acknowledgements—This research has been a major part of ten years of work on solar ponds at the University of Reading, none of which would have been possible but for the continuous support and enthusiasm of Professor Peter Dunn, Head of Engineering Department. His most perceptive comments throughout, together with those of Professor John Hunt before the drafting of this paper, have been invaluable. It is a pleasure also to acknowledge that, throughout this work, Professor Turner's book 'Buoyancy effects in fluids' has been an invaluable source of information, factual, analytical and inspirational. It is hoped that this research has usefully carried forward his view that '... the properties of the "environment" are modified or even produced by the convective elements'.

REFERENCES

1. M. Afeef, Salt gradient solar ponds and desalination, Ph.D. Thesis, University of Reading (1985).
2. M. Afeef and L. B. Mullett, Solar transmission in salt solutions with particular reference to solar ponds, *Solar Wind Technol.* **6**(1), 1–9 (1989).
3. A. Rabl and C. E. Nielsen, Solar ponds for space heating, *Sol. Energy* **17**, 1–12 (1974).
4. H. Weinberger, The physics of the solar pond, *Sol. Energy* **8**(2), 45–56 (1964).
5. H. Tabor, Solar ponds, *Sol. Energy* **27**(3), 181–194 (1981).
6. P. T. Tsilingiris, Analytical and experimental studies on salt gradient solar ponds, Ph.D. Thesis, University of Reading (1985).
7. J. M. Richards, Experiments on the penetration of an interface by buoyant thermals, *J. Fluid Mech.* **II**, 369–384 (1961).
8. J. S. Turner, The behaviour of a stable gradient heated from below, *J. Fluid Mech.* **33**, 183–200 (1968).
9. J. S. Turner, *Buoyancy Effects in Fluids*. Cambridge University Press (1979).
10. P. T. Tsilingiris and L. B. Mullett, The process of loss of internal stability in salt gradient solar ponds, *Int. J. Energy Res.* **13**, 527–536 (1989).
11. A. A. Azhari, Solar energy in Saudi Arabia—with special reference to growth of the lower convecting zone, in the salt gradient solar pond, Ph.D. Thesis, University of Reading (1988).
12. G. Veronis, Penetrative convection, *Aps. J.* **137**, 641–663 (1963).
13. F. Zangrando, D. Munoz and H. Johnstone, Entrainment conditions at the lower interface of a solar pond, *Proceedings of the Conference, International Progress in Solar Ponds*, Mexico (1987).
14. E. M. Sparrow, R. B. Husar and R. J. Goldstein, Observations and other characteristics of thermals, *J. Fluid Mech.* **41**, 793–800 (1970).
15. L. N. Howard, Convection at high Rayleigh number, *Proceedings of the Eleventh Int. Congress Applied Mechanics, Munich*, pp. 1109–1115. Springer, Berlin (1964).
16. A. A. Townsend, Temperature fluctuations over a heated horizontal surface, *J. Fluid Mech.* **5**, 209–241 (1959).
17. J. W. Elder, The unstable thermal interface, *J. Fluid Mech.* **32**, 69–96 (1968).
18. R. W. Griffiths, Entrainment and stirring in viscous plumes, *Phys. Fluids* **A3**(5), 1233–1242 (1991).
19. J. S. Turner, Buoyant plumes and thermals, *Annual Rev. Fluid Mech.* **1**, 29–44 (1969).
20. P. M. Saunders, Penetrative convection in stably stratified fluids, *Tellus* **14**, 177–194 (1962).
21. K. B. Katsaros, W. T. Liu, J. A. Businger and J. E. Tillman, Heat transport and thermal structure in the interfacial boundary layer measured in an open tank of water in turbulent free convection, *J. Fluid Mech.* **83**, 311–335 (1979).
22. A. H. Woodcock, *J. mar. Res.* **4**, 153 (1941).
23. W. G. Spangenberg and W. R. Rowland, Convective circulation in water induced by evaporative cooling, *Phys. Fluids* **4**, 743–750 (1961).
24. J. R. A. Pearson, On convection cells induced by surface tension, *J. Fluid Mech.* **4**, 489–500 (1958).
25. H. E. Huppert and P. F. Linden, On heating a stable salinity gradient from below, *J. Fluid Mech.* **95**, 431–464 (1979).

26. H. Weinberger, Stability criteria for liquid systems with temperature and salt concentration gradients, National Physical Laboratory of Israel publication (1962).
27. G. Veronis, On finite amplitude instability in thermohaline convection, *J. mar. Res.* **26,** 1–17 (1965).
28. H. J. S. Fernando, The formation of a layered structure when a stable salinity gradient is heated from below, *J. Fluid Mech.* **182,** 525–541 (1987).
29. D. J. Tritton, *Physical Fluid Dynamics*. Clarendon Press, Oxford (1988).
30. P. F. Linden and T. G. L. Shirtcliffe, The diffusive interface in double-diffusive convection, *J. Fluid Mech.* **87,** 417–432 (1978).
31. Lord Rayleigh, On convection currents in a horizontal layer of fluid when the higher temperature is on the underside, *Phil. Mag. (6)* **32,** 529–546 (1916).
32. Lord Rayleigh, Investigation of the character of the equilibrium of an incompressible heavy fluid of variable density, *Proc. Lond. Math. Soc.* **XIV,** 170–177 (1883).
33. J. R. Hull and J. M. Mehta, Physical model of gradient zone erosion in thermohaline systems, *Proc. Am. Solar Energy Soc.*, pp. 279–283. Boulder, CO (1986). Later published almost identically in *Int. J. Heat Mass Transfer* **3**(6), 1027–1036 (1987).
34. H. T. Rossby, A study of Benard convection with and without rotation, *J. Fluid Mech.* **36,** 309–335 (1969).
35. J. Gille, Interferometric measurement of temperature gradient reversal in a layer of convecting air, *J. Fluid Mech.* **30,** 371–384 (1967).
36. J. R. Herring, Investigation of problems in thermal convection, *J. Atmos. Sci.* **20,** 325–338 (1963).
37. J. R. Herring, Investigation of problems in thermal convection: rigid boundaries, *J. Atmos. Sci.* **21,** 277–290 (1964).
38. J. W. Elder, The temporal development of a model of high Rayleigh number convection, *J. Fluid Mech.* **35,** 417–437 (1969).